Influence of magnetic field and ionization on gradient driven instability in an E × B plasma

Munish [1,2], Rajat Dhawan[1], Dimple Sharma [1], Hitendra K. Malik[1]*

Abstract

An **E** × **B** plasma is important for various applications including Hall thrusters and magnetic nozzle for long-lasting space propulsion. Such a cross field arrangement in inductively coupled plasma plays vital role in film deposition and etching that are the basic ingredients in semiconductor industries; though in these applications, only the electrons are magnetized which enhance the plasma production and hence, ultimately control the etching aspect ratio and film quality. In the present work, an **E** × **B** plasma is considered where ionization takes place and finite temperature gradient also exists. Specifically, a theoretical model is developed for analysing the effect of magnetic field on the density gradient driven instability. The growth rate of the instability is evaluated as a function of plasma background density, scale length of density gradient, ionization frequency, charge on ions, ion temperature gradient, temperatures of plasma species and magnetic field. To generalize the situation, case of different masses of the ions is also reviewed by considering both the electrons and the ions to be magnetized.

Keywords

E × **B** plasma, Ionization, Temperature of plasma species, Ions' mass, Density gradient driven instabilities.

[1] *Plasma Science and Technology Laboratory, Department of Physics, Indian Institute of Technology Delhi, New Delhi, India*
[2] *Department of Physics, Gargi College, University of Delhi, Delhi, India*
Corresponding author: hkmalik@physics.iitd.ac.in

1. Introduction

Nowadays, Hall thrusters have become a promising device among several propulsion devices because of their superior efficiency and thrust density [1, 2]. Hall thrusters find several important applications in small satellites, commercial space missions and telecommunications satellites [3]. In future, such propulsion devices shall be adopted for orbit topping applications. Therefore, precise information of the physical mechanisms taking place in the plasma of a thruster is requisite to enhance the Hall thruster efficiency. Various physical processes are accompanied with the plasma fluctuations. The fluctuations in the Hall thruster plasma have been measured by Lazurenko et al. [4] adopting electrostatic probes and antennas. Considering the impact of ionization, low-frequency oscillations in a Hall thruster have been studied by Barral et al. [5]. The frequencies of azimuthal and axial propagating plasma disturbance along with the growth rate have been obtained theoretically by Chesta et al. [6]. Along with the process of ionization, an associated low-frequency instability is also identified by them. Litvak et al. [7] have recorded high-frequency instability experimentally in the range of 5 – 10 MHz. In Hall thrusters, plasma is situated under the impact of magnetic field and it remains far from the equilibrium which leads to the conditions for the occurrence of plasma instabilities. The performance of the thruster is influenced by such instabilities, therefore, most of the researchers have given a special emphasis on the investigation of gen-

erated instabilities [8–12]. In the Hall thruster plasma, the instabilities have been demonstrated to trigger by the combination of the density gradients and the magnetic field [13]. A further modification has been observed in the instabilities because of the inhomogeneity of the electron flow, which in turn, leads to the generation of Rayleigh type instability [14]. Low-frequency oscillations are because of the coupling between self-consistent electric field and the ion current, which in turn, leads to Buneman's instability [15]. In annular Hall thruster, Chesta et al. [16] and Parker et al. [17] have detected a different variety of instability, named as rotating spoke instability. By neglecting electron inertia effect, Frias et al. [18] and Smolyakov et al. [19] have obtained the long-wavelength gradient drift instabilities. These instabilities are triggered by the magnetic field and plasma density gradients. In non-Maxwellian plasma, low-frequency sheath instability has been investigated by Starodubtsev et al. [20, 21].

For the sake of simplicity, the impact of ionization and temperature of plasma species have been neglected in most of the studies. In the present study, we have considered finite temperature of both the plasma species and a non-zero ionization rate to investigate the exact behaviour of density gradient driven instability under the effect of several plasma parameters like ion temperature gradient, charge on ions, channel length, plasma background density, etc. We have also considered different masses of the ions to analyse the realistic situations. Both the electrons and ions are assumed to be magnetized in an **E** × **B** system, where a gradient exists in
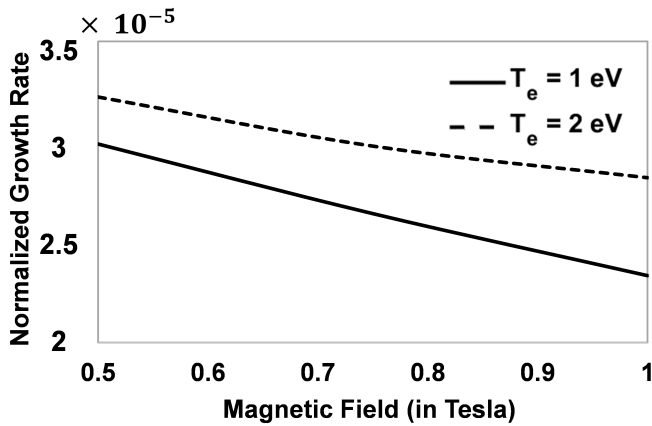
Figure 1. Normalized growth rate of instability as a function of magnetic field (in Tesla) for different temperature of electrons (T_e) in eV, when $d = 5$ m, $\lambda = 5$ cm, $x = \lambda/4$, $n_{e00} = n_{i00} = 10^{18}$m^{-3}, $T_i = 0.3$ eV, $m_i = 1.6 \times 10^{-27}$ kg, $V_{y00} = 10^3$ m/s, $U_{y00} = 10^5$ m/s, $Z = 1$, $\alpha = 10^2$ s^{-1} and $\partial_x T_i = 1$ eV/m.

their temperatures. The temperature gradient has been seen in other fluidic motions [22, 23] and in the plasmas used in magnetic nozzle [24, 25]. Our calculations show that such a plasma is susceptible to the instability. Hence, the present model would help experimentalists conducting experiments smoothly by keeping the system far from the instabilities and will contribute to semiconductor industries.

2. Formulation of the problem

In the present study, both the electrons and ions are assumed to be magnetized in view of the applied magnetic field (**B**) in the z-direction. Since the finite temperature of both these species is considered, a non-zero pressure-gradient term will appear in their fluid equations. Space coordinates are chosen to be varied in the x- and y-directions, i.e. two-dimensional adiabatic approximation has been adopted to investigate the given system. Consequently, the motion of both the electrons and ions will be affected by the $\mathbf{E} \times \mathbf{B}$ drifts.

In the fundamental equations, n_j is the density, T_j is the temperature and m_j is the mass of the electrons ($j = e$) and ions ($j = i$). U and V, respectively, depict the velocities of the electrons and ions. Ze and e are the charges of the ions and electrons, respectively. The un-perturbed part and oscillating part of the densities are represented by (n_{i0}, n_{e0}) and (n_{i1}, n_{e1}), respectively. The x- and y-components of the un-perturbed and oscillating parts of the velocities are expressed as $(V_{x0}, U_{x0}, V_{y0}, U_{y0})$ and $(V_{x1}, U_{x1}, V_{y1}, U_{y1})$, respectively. The electric field has its oscillating value as $\mathbf{E}_1$ and the associated potential is φ_1. The oscillating quantities are taken to vary as $\exp[i(\omega t - ky)]$, where ω is the frequency of oscillations and k is the wavenumber associated with the oscillations of wavelength λ.

The fundamental equations for the given system are the continuity equations and equations of motion for both the electrons and ions. Poisson's equation reveals the relationship of plasma
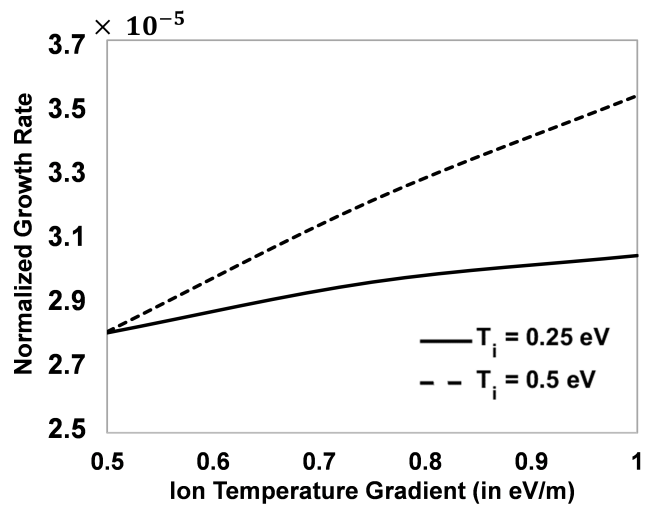

Figure 2. Normalized growth rate of instability as a function of the ion temperature gradient (in eV/m) for different temperature of ions (T_i) in eV, when $d = 5$ m, $\lambda = 5$ cm, $x = \lambda/4$, $n_{e00} = n_{i00} = 10^{18}$m^{-3}, $T_e = 1.5$ eV, $m_i = 1.6 \times 10^{-27}$ kg, $V_{y00} = 10^3$ m/s, $U_{y00} = 10^5$ m/s, $B_0 = 1$ T, $\alpha = 10^2$ s^{-1} and $Z = 1$.

species densities with the electric potential. In linearized form, the said equations read

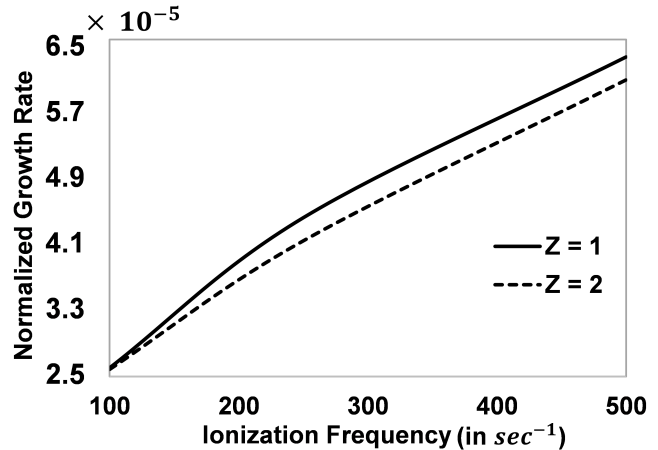**A. For electrons**:
(i) Continuity equation

Figure 3. Normalized growth rate of instability as a function of ionization frequency (in sec^{-1}) for different charge on the ions (Z) when $d = 5$ m, $\lambda = 5$ cm, $x = \lambda/4$, $n_{e00} = n_{i00} = 10^{18}$m^{-3}, $T_i = 0.3$ eV, $T_e = 1.5$ eV, $m_i = 1.6 \times 10^{-27}$ kg, $V_{y00} = 10^3$ m/s, $U_{y00} = 10^5$ m/s, $B = 1$ T and $\partial_x T_i = 1$ eV/m.

$$\partial_t n_{e1} + n_{e0}\partial_x U_{x1} + n_{e0}\partial_y U_{y1} + U_{x1}\partial_x n_{e0} + U_{y0}\partial_y n_{e1}$$

$$= \alpha n_{e0} + \alpha n_{e1} \qquad (1)$$

(ii) x-component of equation of motion

$$\partial_t U_{x1} + U_{y0} \cdot \partial_y U_{x1} = \frac{e}{m_e} \cdot \partial_x \varphi_1 - \frac{e}{m_e} \cdot (U_{y0} + U_{y1})(B_0)$$

$$-\frac{2T_e}{m_e n_e} \cdot \partial_x n_{e0} - \frac{2T_e}{m_e n_e} \cdot \partial_x n_{e1} - \frac{2}{m_e}\partial_x T_e - \alpha U_{x1} \quad (2)$$

(iii) y-component of the equation of motion

$$\partial_t U_{y1} + U_{x1}\cdot\partial_x U_{y0} + U_{y0}\cdot\partial_y U_{y1}$$

$$= \Omega_e U_{x1} - \frac{2T_e}{m_e n_e}\cdot\partial_y n_{e1} + \frac{e}{m_e}\cdot\partial_y \varphi_1 - \alpha U_{y0} - \alpha U_{y1} \quad (3)$$

B. For ions:
(iv) Continuity equation

$$\partial_t n_{i1} + n_{i0}\partial_x V_{x1} + V_{x1}\partial_x n_{i0} + n_{i0}\partial_y V_{y1} + V_{y0}\partial_y n_{i1} = \alpha n_{i0} + \alpha n_{i1} \quad (4)$$

(v) x-component of the equation of motion

$$\partial_t V_{x1} + V_{y0}\partial_y V_{x1} = -\frac{Ze}{m_i}\partial_x \varphi_1 + \frac{Ze}{m_i}\cdot(V_{y0} + V_{y1})(B_0)$$

$$-\frac{2T_i}{m_i n_i}\cdot(\partial_x n_{i0} + \partial_x n_{i1}) - \frac{2}{m_i}\partial_x T_i - \alpha V_{x1} \quad (5)$$

(vi) y-component of the equation of motion

$$\partial_t V_{y1} + V_{x1}\partial_x V_{y0} + V_{y0}\partial_y V_{y1} = -\frac{Ze}{m_i}\cdot\partial_y \varphi_1 - \frac{Ze}{m_i}\cdot V_{x1}(B_0)$$

$$-\frac{2T_i}{m_i n_i}\cdot\partial_y n_{i1} - \alpha V_{y0} - \alpha V_{y1} \quad (6)$$

In Eqs. (1)-(6), ∂_t, ∂_x and ∂_y are the first-order derivatives with respect to t, x and y, respectively. α is the ionization frequency. Take $\Omega_i = ZeB_0/m_i$ and $\Omega_e = eB_0/m_e$ as the ion-cyclotron and electron-cyclotron frequencies, respectively, $\acute{A} = i\omega - \alpha - ikU_{y0}$, $\acute{B} = 1 + (2T_e k^2/\acute{A}m_e\omega)$ and ω_e as the electron-plasma frequency, given by $(n_{e0}e^2/m_e\varepsilon_0)^{1/2}$. Also take $A_1 = i\omega - \alpha - ikV_{y0}$, $B_1 = 1 + 2T_i k^2/A_1 m_i\omega$ and ω_i as the ion-plasma frequency, given by $(n_{i0}e^2/m_i\varepsilon_0)^{1/2}$. Poisson's equation which reveals the relationship between the densities of the plasma species and the electric potential is stated as follows

$$\varepsilon_0(\partial_x^2 + \partial_y^2)\varphi_1 = e(n_{e1} - Zn_{i1}) \quad (7)$$

Using Eq. (7), we have the following expression

$$(\partial_x^2\varphi_1 - k^2\varphi_1) + \partial_x^2\varphi_1\left[\frac{n_{e0}e^2}{X_1\acute{A}\acute{B}\varepsilon_0 m_e\omega_e} - \frac{Z^2 e^2 n_{i0}}{S_1 A_1 B_1 m_i\omega_i\varepsilon_0}\right]$$

$$+k^2\varphi_1\left(\frac{Z^2 e^2 n_{i0}\omega_i}{A_1 B_1 m_i\Omega_i^2\varepsilon_0}\right) + \varphi_1\left[\frac{ZeikP_1\omega_i}{Q_1 m_i\Omega_i^2} - \frac{ikT_1\omega_e e}{U_1 m_e\Omega_e^2} + \frac{V_1 e^2 B_0 ik}{W_1 X_1 m_e^2\omega_e}\right]$$

$$+\left[-\frac{\alpha n_{e0}e}{\acute{A}\acute{B}\varepsilon_0} + \frac{Ze\alpha n_{i0}}{A_1 B_1\varepsilon_0} - \frac{2T_i P_1}{Q_1 m_i n_{i0}\Omega_i}\right]\partial_x n_{io}$$

$$-\frac{2P_1}{Q_1 m_i\Omega_i}\partial_x T_i - \frac{2T_i P_1 ZeB_0}{Q_1 m_i^2\Omega_i^2 n_{i0}}\partial_x n_{i0} - \frac{2P_1 ZeB_0}{Q_1 m_i^2\Omega_i^2}\partial_x T_i$$

$$+\frac{2T_i Zeik}{A_1 B_1 m_i\Omega_i\varepsilon_0}\partial_x n_{i0} + \frac{2ikn_{i0}Ze}{A_1 B_1 m_i\Omega_i\varepsilon_0}\partial_x T_i + \frac{2ikZ^2 e^2 T_i B_0}{A_1 B_1 m_i^2\Omega_i^2\varepsilon_0}\partial_x n_{i0}$$

$$+\frac{2ikZ^2 e^2 n_{i0}B_0}{A_1 B_1 m_i^2\Omega_i^2\varepsilon_0}\partial_x T_i + \frac{2ikn_{i0}Ze}{A_1 B_1 m_i\Omega_i^2\varepsilon_0}\partial_x T_i\partial_x V_{y0} + \frac{2R_1 KT_i}{S_1^2 en_{i0}}\partial_x n_{i0}$$

$$+\frac{2V_1 T_e}{W_1 X_1 m_e n_{e0}\omega_e}\partial_x n_{e0} - \frac{2P_1 T_i ik\omega_i}{Q_1 m_i\Omega_i^2} + \frac{2V_1 T_e ikB_0 e}{W_1 X_1 m_e^2\omega_e^2}\right] = 0 \quad (8)$$

In the acceleration channel, the electron density, ion density, electron drift velocity and ion drift velocity are taken to follow the expression

$$F_0 = F_{00}e^{-10(\frac{x}{d})^2} \quad (9)$$

Here, the peak value of n_{e0}, n_{i0}, U_0 and V_0 is represented by F_{00}. Using the above velocities and densities profiles, the un-perturbed part of Eq. (9) has been solved to calculate the growth rate of the instabilities. This led to the following dispersion equation

$$G_1\omega^6 + G_2\omega^5 + G_3\omega^4 + G_4\omega^3 + G_5\omega^2 + G_6\omega + G_7 = 0 \quad (10)$$

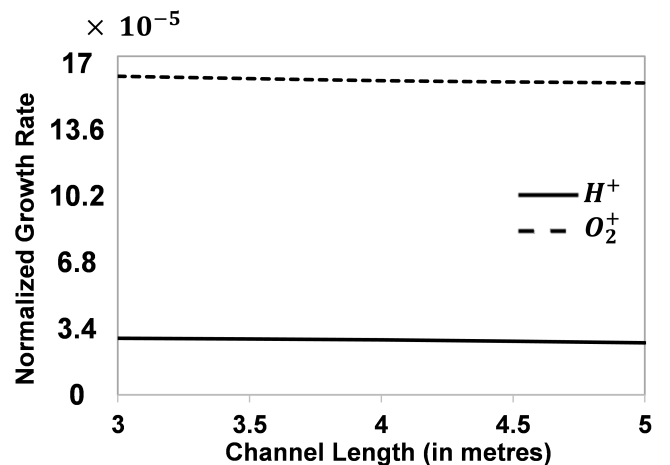The coefficients and the constants used in Eq. (10) are shown in appendix

Figure 4. Normalized growth rate of instability as a function of channel length (in metres) for different masses of ions when $\lambda = 5$ cm, $x = \lambda/4$, $n_{e00} = n_{i00} = 10^{18}$m^{-3}, $T_i = 0.3$ eV, $T_e = 1.5$ eV, $V_{y00} = 10^3$ m/s, $U_{y00} = 10^5$ m/s, $B = 1$ T, $\alpha = 10^2$ s^{-1}, $Z = 1$ and $\partial_x T_i = 1$ eV/m.
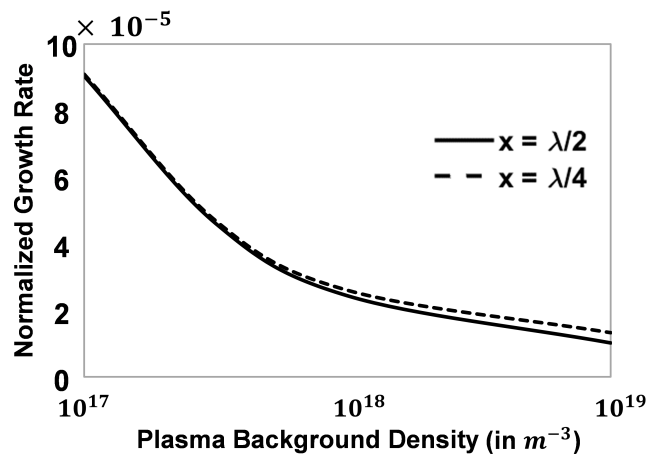
Figure 5. Normalized growth rate of instability as a function of plasma background density (in m^{-3}) for different values of x when $d = 5$ m, $\lambda = 5$ cm, $T_i = 0.3$ eV, $T_e = 1.5$ eV, $m_i = 1.6 \times 10^{-27}$ kg, $V_{y00} = 10^3$ m/s, $U_{y00} = 10^5$ m/s, $B = 1$ T, $\alpha = 10^2$ s^{-1}, $Z = 1$ and $\partial_x T_i = 1$ eV/m.

3. Results

The growth rate of the instability has been determined from the numerical solution of the dispersion equation (10). Numerical solutions and simulations have been used in other areas also [26–28]. In Figs. (1) -(5), normalised growth rate with the ion-plasma frequency (ω_i) has been plotted by taking same gradient in the temperature for both the ions and electrons. Variation of the growth rate as a function of magnetic field (in Tesla) has been portrayed in Fig. 1 for different values of the electrons temperature (T_e) in eV. The magnitude of the normalized growth rate is reduced with an increased magnetic field whereas it is raised for higher temperature of the electrons. The difference in the magnitude of the growth rate for different electron temperature is found to be more for larger values of the magnetic field. The reduction in the growth rate with the magnetic field is the similar observation as made by Pachauri et al. [29], who considered dust in the system, Malik et al. [30], Tyagi et al. [31,32] and Munish et al. [33].

The variation of the normalized growth with the ion temperature gradient (in eV/m) has been investigated and depicted in Fig. 2 for different values of ion temperature (T_i) in eV. The magnitude of the normalized growth rate is found to increase with an increased ion temperature gradient, similarly to the case of Munish et al. [33]; the same is the case with the higher temperature of ions. The difference in the magnitude of growth rate for different ion temperatures is enhanced very significantly for the increasing ion temperature gradient. These results show that the gradient in the ion temperature supports the instability that is driven by the density gradient. Actually, the higher temperature gradient plays a similar role as the larger density gradient, and it is plausible that the coupling of free energy is more with the oscillations when the ions carry higher thermal energy.

The response of the normalized growth rate of instability for the ionization frequency has been analysed through Fig. 3 for different values of charge on the ions (Z). The instability is found to grow faster in the plasma having larger ionization or the ionization frequency. However, in the plasma having doubly charged ions, the growth falls down and this effect is much significant for the larger ionization. The reduction in the growth rate with the higher charge of the ions is the similar observation as made by Pachauri et al. [29], Malik et al. [30], Tyagi et al. [31,32] and Munish et al. [33].

In order to see the role of scale length of the density gradient on the evolution of instability in different kinds of plasmas, we have plotted the growth rate with respect to the channel length for plasmas having H$^+$ ions or O^{2+} ions. The growth rate is found to reduce slightly with the larger scale length. Since larger scale length means weaker density gradient, the lower growth rate of the instability is expected as it is driven by the density gradient. Moreover, the instability attains much higher growth rate in the plasma carrying heavy ions. This might be attributed to the higher coupling of the free energy to the oscillations in the presence of heavier ions.

Finally, the effect of background plasma density is studied on the growth of instability in Fig. 5. In view of the density gradient present in the plasma, the growth rate is also evaluated at different positions, i.e. x, in terms of the wavelength of the wave. The instability is found to grow slowly in the plasma having the higher density. In the presence of higher background density, the role of the gradients seems to be weakened due to the weak coupling of free energy with the oscillations and hence, the instability grows smaller. Further, the growth rate at $x = \lambda/4$ is higher than the rate at $= \lambda/2$. This is in view of different densities at these positions and the effective lower density gradient due to the larger scale length. The pressure gradient developed due to the temperature gradient has been shown to play vital role in magnetic nozzles for the effective space propulsion [24,25]. Also, the Rayleigh-Taylor instability in the presence of dusty plasma in Hall thrusters has been found to be influenced by the density gradient [30-33]. Since dust grains carry a huge charge and different mass from the ions and electrons, our results concerning the charge and mass of the ions would also be quite useful in Hall thrusters in addition to magnetic nozzles. Also inductively coupled plasma along with such a cross field ($\mathbf{E} \times \mathbf{B}$) arrangement has been used for etching [34–36], film deposition [37–39] etc. in semiconductor industries. However, in these applications, only the electrons are magnetized which enhance the plasma production and hence, ultimately control the film quality and etching aspect ratio. In view of this, the current model would enable the experimentalists to conduct experiments smoothly as they can keep the system far from the instabilities by generating plasma with the required properties.

4. Conclusion

In the present magnetized ($\mathbf{E} \times \mathbf{B}$) plasma system having temperature gradient, instability was investigated numerically

under the effect of finite temperature of plasma species and a non-zero ionization frequency. The normalized magnitude of the growth rate of instability was found to increase with the increased electron temperature, ion temperature, ion temperature gradient, ionization frequency and mass of the ion, whereas the growth is reduced with the enhanced plasma background density, scale length of density gradient, charge on the ions and the magnetic field. The finding of this work shall play an imperative role in the technologies like electric propulsion and magnetized plasma sources used in surface processing.

Conflict of interest statement:
The authors declare that they have no conflict of interest.

Appendix

The coefficients and the constants used in Eq. (10) are given as below

$$P_1 = \frac{2Z^2e^2ikn_{i0}B_0}{A_1B_1m_i\Omega_i\varepsilon_0} + \frac{Z^3e^3ikn_{i0}B_0^2}{A_1B_1m_i^2\Omega_i^2\varepsilon_0} + \frac{Z^2e^2ikn_{i0}B_0}{A_1B_1m_i\Omega_i^2\varepsilon_0}\partial_xV_{y0},$$

$$Q_1 = 1 + \frac{2ZeB_0}{m_i\Omega_i} + \frac{Z^2e^2B_0^2}{m_i^2\Omega_i^2} + \frac{ZeB_0}{m_i\Omega_i^2}\partial_xV_{y0},$$

$$R_1 = \frac{\Omega_i}{\omega_i^2}\partial_x^2V_{y0} + \frac{ZeB_0}{m_i\omega_i^2}\partial_x^2V_{y0},$$

$$S_1 = 1 + \frac{\Omega_i^2}{\omega_i^2} + \frac{2ZeB_0\Omega_i}{m_i\omega_i^2} + 2\frac{\Omega_i}{\omega_i^2}\partial_xV_{y0} + \frac{Z^2e^2B_0^2}{m_i^2\omega_i^2},$$

$$T_1 = \frac{ikn_{e0}e^2B_0}{\acute{A}\acute{B}m_e\Omega_e^2\varepsilon_0}\partial_xU_{y0} + \frac{2ikn_{e0}e^2B_0}{\acute{A}\acute{B}m_e\Omega_e\varepsilon_0} + \frac{ikn_{e0}e^3B_0^2}{\acute{A}\acute{B}m_e^2\Omega_e^2\varepsilon_0},$$

$$U_1 = 1 - \frac{eB_0}{m_e\Omega_e^2}\partial_xU_{y0} + \frac{2eB_0}{m_e\Omega_e},$$

$$T_1 = \frac{n_{e0}e\Omega_e}{\acute{A}\acute{B}\varepsilon_0\omega_e^2}\partial_x^2U_{y0} + \frac{n_{e0}B_0e^2}{\acute{A}\acute{B}\varepsilon_0m_e\omega_e^2}\partial_x^2U_{y0}$$

$$W_1 = 1 + \frac{4\Omega_e^2}{\omega_e^2} - \frac{2\Omega_e}{\omega_e^2}\partial_xU_{y0}$$

$$X_1 = 1 + \frac{4\Omega_e^2}{\omega_e^2} - \frac{eB_0}{m_e\omega_e^2}\partial_xU_{y0},$$

$$G_1 = QLiF, G_2 = B_2iLF + QL\acute{X} + QKiF,$$

$$G_3 = A_2LFi + B_2L\acute{X} + B_2KFi + QL\acute{Y} + QK\acute{X} + RC_2Fi,$$

$$G_4 = A_2L\acute{X} + A_2KFi + B_2L\acute{Y} + QL\acute{Z} + Q\acute{Y}K + RC_2\acute{X} - RBNiF + PIC_2Li,$$

$$G_5 = A_2L\acute{Y} + A_2K\acute{X} + B_2L\acute{Z} + B_2K\acute{Y} + QK\acute{Z} + RC_2\acute{Y}$$

$$-RBN\acute{X} + PIC_2Ki - BNLPIi + PIDC_2L,$$

$$G_6 = A_2L\acute{Z} + A_2K\acute{Y} + B_2K\acute{Z} + RC_2\acute{Z} - RBN\acute{Y}$$

$$-BNKPIi + PIDC_2K - PIDBNL,$$

$$G_7 = A_2K\acute{Z} - RBN\acute{Z} - PIDBNK,$$

$$A_2 = MN - QN^2, B_2 = Mi - 2iNQ, C_2 = AN - Bi$$

$$\acute{X} = iG = CF + EF, \acute{Y} = iH + CG + EG, \acute{Z} = CH + EH,$$

$$R = \frac{4T_eik^2\alpha n_{e0}e}{m_e\Omega_e^2\varepsilon_0}$$

$$P = \frac{2T_eke}{m_e\varepsilon_0}\partial_xn_{e0}$$

$$N = \alpha - ikV_{y0}$$

$$Q = \frac{2T_iik\Lambda}{\acute{Q}m_i\Omega_i^2}$$

$$M = \frac{Ze\alpha n_{i0}}{\varepsilon_0} + \frac{2T_iZeik}{m_i\Omega_i\varepsilon_0}\partial_xn_{i0}$$

$$+\frac{2ikZ^2e^2T_iB_0}{m_i^2\Omega_i^2\varepsilon_0}\partial_xn_{i0} + \frac{2ikn_{i0}Ze}{m_i\Omega_i\varepsilon_0}\partial_xT_i$$

$$+\frac{2Z^2e^2ikn_{i0}B_0}{m_i^2\Omega_i^2\varepsilon_0}\partial_xT_i + \frac{2ikn_{i0}Ze}{m_i\Omega_i^2\varepsilon_0}\partial_xV_{y0}\partial_xT_i$$

$$+\Lambda[-\frac{2T_i}{\acute{Q}m_in_{i0}\Omega_i}\partial_xn_{i0} - \frac{2T_iZeB_0}{\acute{Q}m_i^2\Omega_i^2n_{i0}}$$

$$-\frac{2}{\acute{Q}m_i}\partial_xT_i - \frac{2ZeB_0}{\acute{Q}m_i^2\Omega_i^2}\partial_xT_i]$$

$$\acute{Q} = 1 + \frac{2ZeB_0}{m_i\Omega_i} + \frac{Z^2e^2B_0^2}{m_i^2\Omega_i^2} + \frac{ZeB_0}{m_i\Omega_i^2}\partial_xV_{y0},$$

$$L = i + \frac{2T_e k^2}{m_e \Omega_e^2},$$

$$K = \frac{2T_e k^2 \alpha}{m_e \Omega_e^2} - \frac{2T_e k^2 ik U_{y0}}{m_e \Omega_e^2} - ik U_{y0} - \alpha,$$

$$J = 2eB_0 \Omega_e m_e + 2e^2 B_0^2 - 2eB_0 m_e \partial_x U_{y0},$$

$$I = m_e n_{e0} \Omega_e^2,$$

$$H = -ik U_{y0} m_e n_{e0} \Omega_e^2 D + \alpha D m_e n_{e0} \Omega_e^2 - (k^2 U_{y0} + \alpha^2) * 2 T_e k^2 n_{e0},$$

$$G = -\alpha i m_e n_{e0} \Omega_e^2 + i D m_e n_{e0} \Omega_e^2 - 4 T_e k^3 n_{e0} U_{y0} + k U_{y0} m_e n_{e0} \Omega_e^2,$$

$$F = -2T_e k^2 n_{e0} - m_e n_{e0} \Omega_e^2,$$

$$E = \frac{e^2 B_0 - e B_0 m_e \partial_x U_{y0}}{m_e^2 \Omega_e},$$

$$D = -\alpha - ik V_{y0},$$

$$C = \alpha - ik V_{y0}$$

$$B = ik V_{y0} + \alpha + \frac{2T_i k^3 V_{y0}}{m_i \Omega_i^2} - \frac{2T_i k^2 \alpha}{m_i \Omega_i^2},$$

$$A = i + \frac{2T_i ik^2}{m_i \Omega_i^2},$$

$$\Lambda = \frac{2Z^2 e^2 ik n_{i0} B_0}{m_i \Omega_i \varepsilon_0} + \frac{Z^2 e^2 ik n_{i0} B_0}{m_i \Omega_i^2 \varepsilon_0} \partial_x V_{y0}$$

References

[1] V. V. Zhurin, H.R. Kaufman, and R. S. Robinson. *Plasma Sources Science and Technology*, **8**:R1, 1999.

[2] E. Y. Choueiri. *Physics of Plasmas*, **8**:1411, 2001.

[3] J. P. Boeuf. *Journal of Applied Physics*, **121**:11101, 2017.

[4] A. Lazurenko, V. Vial, M. Prioul, and A. Bouchoule. *Physics of Plasmas*, **12**:13501, 2005.

[5] S. Barral, K. Makowski, Z. Peradzy´nski, and M. Dudeck. *Physics of Plasmas*, **12**:73504, 2005.

[6] E. Chesta, N.B. Meezan, and M. A. Cappelli. *Journal of Applied Physics*, **89**:3099, 2001.

[7] A. A. Litvak, Y. Raitses, and N. J. Fisch. *Physics of Plasmas*, **11**:1701, 2004.

[8] E. Fernandez, M. K. Scharfe, C. A. Thomas, N. Gascon, and M. A. Cappelli. *Physics of Plasmas*, **15**:12102, 2008.

[9] S. Sen, A. Fukuyama, and F. Honary. *Journal of Atmospheric and Solar-Terrestrial Physics*, **72**:938, 2010.

[10] S. Singh and H.K. Malik. *IEEE Transactions on Plasma Science*, **39**:1910, 2011.

[11] S. Singh, H. K. Malik, and Y. Nishida. *Physics of Plasmas*, **20**:102109, 2013.

[12] H. K. Malik and S. Singh. *Physics of Plasmas*, **20**:52115, 2013.

[13] Y. V Esipchuk and G. N. Tilinin. *Soviet physics. Technical physics(Engl. Transl.)*, **21**, 1976.

[14] H. K. Malik and S. Singh. *Physical Review E*, **83**:36406, 2011.

[15] S. Chable and F. Rogier. *Physics of Plasmas*, **12**:33504, 2005.

[16] E. Chesta, C. M. Lam, N. B. Meezan, D. P. Schmidt, and M. A. Cappelli. *IEEE Transactions on Plasma Science*, **29**:582, 2001.

[17] J. B. Parker, Y. Raitses, and N. J. Fisch. *Applied Physics Letters*, **97**:91501, 2010.

[18] W. Frias, A. I. Smolyakov, I. D. Kaganovich, and Y. Raitses. *Physics of Plasmas*, **19**:72112, 2012.

[19] A. I. Smolyakov, W. Frias, Y. Raitses, and N. J. Fisch. *Proc. 32nd Int. Electr. Propulsion Conf.*, , 2011.

[20] M. Starodubtsev, M. Kamal-Al-Hassan, H. Ito, N. Yugami, and Y. Nishida. *Physical Review Letters*, **92**:45003, 2004.

[21] M. Starodubtsev, M. Kamal-Al-Hassan, H. Ito, N. Yugami, and Y. Nishida. *Physics of Plasmas*, **13**:12103, 2006.

[22] L. Malik and A. Tevatia. *Defence Science Journal*, **71**:137, 2021.

[23] L. Malik, S. Rawat, M. Kumar, and A. Tevatia. *Materials Today: Proceedings*, **38**:191, 2021.

[24] L. Malik, M. Kumar, and I. V. Singh. *IEEE Transactions on Plasma Science*, **49**:2227, 2021.

[25] L. Malik. *Propulsion and Power Research*, **11**:171, 2022.

[26] L. Malik, A. Escarguel, M. Kumar, A. Tevatia, and R.S. Sirohi. *Laser Physics Letters*, **18**:086003, 2021.

[27] L. Malik. *Optics and Laser Technology*, **132**:106485, 2020.

[28] L. Malik and A. Escarguel. *Europhysics Letters: EPL*, **124**:64002, 2019.

[29] S. Pachauri, J. Chaudharya, and K. P. Misra. *Plasma Research Express*, **4**:025004, 2022.

[30] H. K. Malik, J. Tyagi, and D. Sharma. *AIP Advances*, **9**:055220, 2019.

[31] J. Tyagi, S. Singh, and H.K. Malik. *Journal of Theoretical and Applied Physics*, **12**:39, 2018.

[32] J. Tyagi, D. Sharma, and H. K. Malik. *Journal of Theoretical and Applied Physics*, **12**:227, 2018.

[33] Munish, R. Dhawan, R. Kumar, and H.K. Malik. *Journal of Taibah University for Science*, **16**:725, 2022.

[34] R. J. Shul, G. B. McClellan, S. A. Casalnuovo, D. J. Rieger, S. J. Peartona nd C. Constantine, C. Barratt, R. F. Karlicek Jr, C. Tran, and M. Schurman. *Applied Physics Letters*, **69**:1119, 1996.

[35] E. R. Parker, B. J. Thibeault, M. F. Aimi, M. P. Rao, and N. C. MacDonald. *Journal of the Electrochemical Society*, **152**:C675, 2005.

[36] D. S. Rawala, H. K. Malik, V. R. Agarwal, A. K. Kapoor, B. K. Sehgal, and R. Muralidharan. *IEEE Transactions on Plasma Science*, **40**:2211, 2012.

[37] J. Li, S. J. Kim, S. Han, and H. Chae. *Surface and Coatings Technology*, **422**:127514, 2021.

[38] S. Kumar, A. Malik, D. S. Rawal, S. Vinayak, and H. K. Malik. *Defence Science Journal*, **68**:572, 2018.

[39] S. Kumara, D. S. Rawal, H. K. Malik, R. Sanwal, S. A. Khan, and S. Vinayak. *Journal of Theoretical and Applied Physics*, **13**:299, 2019.